*Research Journal of Pharmaceutical Sciences*_____ __ISSN 2319 – 555X
Vol. **14(2),** 38-51, December **(2025)** *Res. J. Pharmaceutical Sci.*

Therapeutic Potential of Ebselen-Driven Wound Repair in Mercury-Induced Cell Injury in NRK52E Renal Epithelial Cells

Pragati Kumari Gupta[*] and Hafizurrahman
Department of Zoology, Maharani Janki Kunwar College, Bettiah, West Champaran, Bihar-845438, India
pragatikg9@gmail.com

Available online at: www.isca.in, www.isca.me
Received 4th November 2025, revised 30th November 2025, accepted 25th December 2025

Abstract

Mercury, a toxic environmental pollutant, is readily available in the biogeochemical cycle and poses serious health risks even at trace levels due to its tendency to bioaccumulate. Among its forms, methylmercury (MeHg) is the most toxic, capable of crossing both the placental barrier and blood-brain barrier. This study investigates the cellular toxicity of MeHg on normal rat kidney epithelial cells (NRK52E) and evaluates the protective potential of Ebselen, an organic selenium compound with antioxidant and metal-chelating properties. NRK52E cells were exposed to 0.1 µM and 1 µM concentrations of MeHg, both alone and in combination with 10 µM Ebselen. Multiple assays including wound healing for cell migration, DCFDA for reactive oxygen species (ROS) generation, Luminex multiplex assay for key kidney toxicity markers, invasion assay and cell cycle analysis were performed to assess the extent of toxicity and protection. MeHg exposure led to a significant increase in ROS levels, accompanied by dysregulation of cell adherence and wound healing. These molecular changes were associated with disrupted cell behaviour, impaired wound healing, and altered cell cycle progression, all indicating cellular toxicity. However, co-treatment with Ebselen significantly reversed these effects. ROS levels were reduced and cell cycle distribution improved. Ebselen's ability to restore cellular homeostasis demonstrates its strong protective effect against MeHg-induced nephrotoxicity. This study highlights the potential of Ebselen as a therapeutic agent for mitigating mercury-induced kidney cell damage. It emphasizes the importance of early detection of nephrotoxic effects and timely antioxidant intervention to prevent long-term renal impairment caused by environmental toxins like MeHg.

Keywords: Methylmercury, MTT assay, DCFDA-ROS, Ebselen.

Introduction

Mercury (Hg) is a widespread environmental pollutant that exerts profound nephrotoxic effects, particularly in its methylated form, methylmercury (MeHg), which accumulates in renal tissues. MeHg disrupts the extracellular matrix, impairs cell adhesion, and promotes epithelial-to-mesenchymal transition (EMT), leading to progressive renal injury[1,2]. Oxidative stress is a key pathogenic driver of these events, damaging cytoskeletal integrity and intercellular junctions[3,4].

Ebselen (2-phenyl-1,2-benzisoselenazol-3(2H)-one) is an organoselenium compound with glutathione peroxidase–mimicking activity that scavenges reactive oxygen species (ROS) and protects against heavy-metal–mediated cytotoxicity[5]. Preclinical studies suggest that Ebselen modulates redox homeostasis, inhibits inflammatory cascades, and prevents EMT-associated fibrosis[6].

This study investigates whether Ebselen can mitigate cellular injury by MeHg-induced nephrotoxicity in NRK52E renal epithelial cells and promote wound healing. We hypothesized that Ebselen would (1) reduce ROS production, (2) preserve epithelial phenotype by maintaining E-cadherin expression and suppressing vimentin, and (3) enhance wound healing and repair capacity, ultimately protecting against functional injury.

Materials and Methods

Cell culture and treatmeant: NRK52E rat kidney epithelial cells (ATCC, USA) were cultured in Dulbecco's Modified Eagle Medium (DMEM; Gibco, Thermofisher Scientific, USA) supplemented with 10% fetal bovine serum (FBS), 1% penicillin–streptomycin, and maintained at 37°C in 5% CO_2 . Cells were treated with Methylmercury (MeHg) (Sigma-Aldrich, USA) at 0, 0.5, 1 ,5 and 10 µM for 24 h, either alone or co-treated with Ebselen (10 µM), freshly prepared in Dimethyl sulfoxide (DMSO) (<0.1% final concentration).

Kidney toxicity panel: Molecular analysis: Cell culture supernatants were collected after Methylmercury and Ebselen treatment in doses as discussed in the cell culture methodology. Collected samples were analyzed using the Luminex mutliplex assay for key markers of renal cell injury (Thermo Fisher, USA). This bead-based immunoassay panel used xMAP technology to detect multiple proteins at the same time. The panel consisted of protein biomarkers namely Clusterin, MCP-1 (Monocyte Chemoattractant Protein-1), KIM-1 (Kidney Injury Marker-1), IL-18 (Interleukin-18) and OPN (Osteopontin).

Reactive oxygen species measurement (ROS): DCFDA Assay: Intracellular ROS levels were quantified using 2',7'-

dichlorodihydrofluorescein diacetate (DCFDA, Thermo Fisher, USA). After treatment, cells were incubated with 10µM DCFDA for 30 min in the dark and fluorescence was recorded at 485/535 nm.

Wound healing assay/ Scratch assay: A scratch assay was performed to assess cell migration. Confluent monolayers were scratched with a sterile pipette tip, washed with PBS to remove debris, and incubated under treatment conditions of the experiment. Images were captured at 0 and 24h using an inverted microscope (Olympus IX71), and wound closure percentage was quantified using ImageJ.

Invasion assay: Invasiveness was determined using Matrigel-coated Transwell chambers (8 µm pores, Corning). Cells were seeded in serum-free medium in the upper chamber, with 10% FBS in the lower chamber as chemoattractant. After 24 h, non-invading cells were removed and invading cells were fixed, stained, and counted.

Immunocy to chemistry: Cells were fixed in 4% paraformaldehyde, permeabilized with 0.1% Triton X-100, and incubated with primary antibodies against E-cadherin and vimentin (Cell Signaling Technology), followed by Alexa Fluor–conjugated secondary antibodies. Fluorescence was visualized using a confocal microscope (Leica TCS SP8).

Cell cycle assay: Cell Signaling Multiplex Assay was done by Cell Cycle Analysis Kit ab287852 (Abcam). Cells were collected and fixed in 70% ethanol at -4°C, to permeabilize the cell membrane. Cells were treated with RNase A to digest RNA, ensuring that only the DNA content is measured accurately and incubated with a DNA-binding fluorescent dye Propidium Iodide. The stained cells were run through a flow cytometer. The instrument measured the fluorescence intensity individual cells. The data were plotted as a histogram of cell count versus fluorescence intensity (DNA content). Computer algorithms were then used to calculate the percentage of cells in the G0/G1, S, and G2/M phases based on the distinct fluorescence peaks.

Statistical analysis: All experiments were performed in triplicate (n = 3). Data are expressed as mean ± SD. One-way ANOVA followed by Tukey's post hoc test was used for comparisons. $p < 0.05$ was considered statistically significant.

Results and Discussion

MeHg significantly decreased NRK52E cell viability and increased ROS in a dose-dependent manner: When NRK52E cells grown in DMEM-F12 medium were exposed to varying concentrations of methylmercury (MeHg) to assess dose-dependent cytotoxic effects, cellular disintegration was clearly visible. Higher concentrations of MeHg caused pronounced cellular damage, including loss of adhesion and altered morphology[7]. Co-treatment with Ebselen significantly reduced MeHg-induced toxicity, preserving cellular integrity[8] (Figure-1a-f).

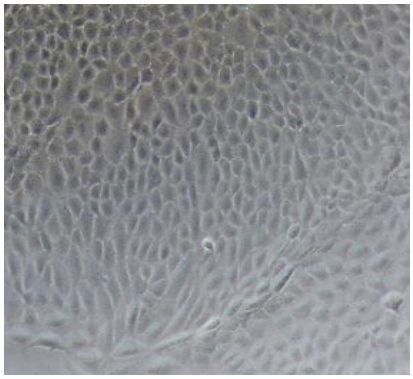

a) Control.

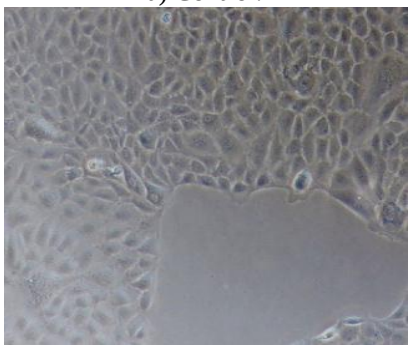

b) 0.5 µM MeHg.

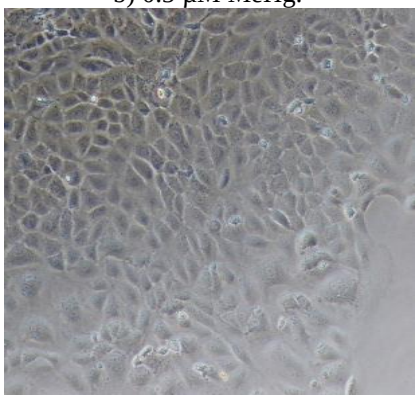

c) 1.0 µM MeHg.

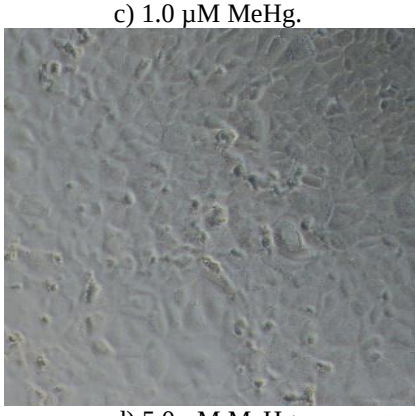

d) 5.0 µM MeHg.

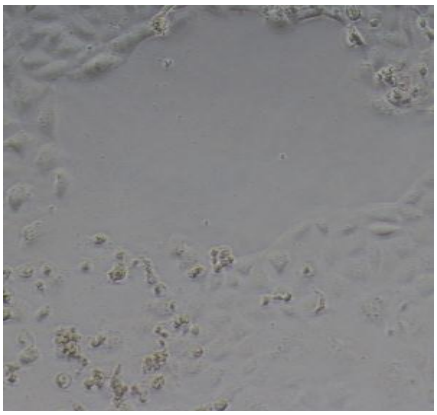

e) 10.0 µM MeHg.

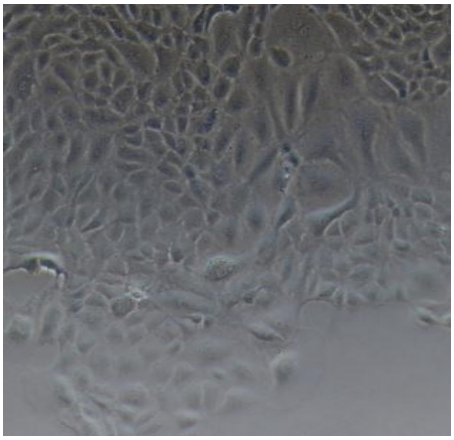

f) 1 µM MeHg + 10 µM Ebselen.

Figure-1(a-f): NRK52E rat kidney epithelial cells were grown in laboratory conditions and exposed to different amounts of methylmercury (MeHg) to see how it affects cell health. As the dose of MeHg increased, the cells showed more signs of damage, they lost their ability to stick to the surface and their normal shape became distorted. When the cells were treated with Ebselen at the same time as MeHg, cytotoxic effects were significantly reduced.

Intracellular ROS levels were measured to assess oxidative stress following exposure to increasing concentrations of MeHg and the potential protective role of Ebselen. As expected, control cells exhibited baseline ROS levels. Treatment with 0.5 µM MeHg resulted in a noticeable increase in ROS compared with control, and a further increase was observed at 1 µM MeHg, demonstrating a clear dose-dependent induction of oxidative stress[9]. Co-treatment with 1 µM MeHg and 10 µM Ebselen markedly reduced ROS levels relative to MeHg alone, indicating a strong antioxidant and protective effect of Ebselen against MeHg-induced oxidative injury[10]. Ebselen alone produced ROS values comparable to control, confirming that it does not independently induce oxidative stress at the tested concentration. As anticipated, H_2O_2 treatment produced the highest fluorescence signal, validating the assay as a positive oxidative stress control[11]. The ROS data demonstrate that MeHg induces oxidative stress in NRK-52E cells in a concentration-dependent manner, consistent with its known mechanism of toxicity involving disruption of redox balance and thiol depletion[12,13]. Importantly, the significant reduction in ROS upon co-treatment with Ebselen indicates that Ebselen effectively mitigates MeHg-mediated oxidative injury, most likely through its glutathione peroxidase–mimetic activity and ability to neutralize peroxides[14,15]. The absence of ROS elevation in cells exposed to Ebselen alone confirms that Ebselen does not act as a pro-oxidant under the tested conditions. The strong ROS signal observed in the H_2O_2 group validates the specificity and sensitivity of the assay. Together, these findings support a protective antioxidant role for Ebselen against MeHg-induced oxidative stress in renal epithelial cells[16,17] (Figure-2).

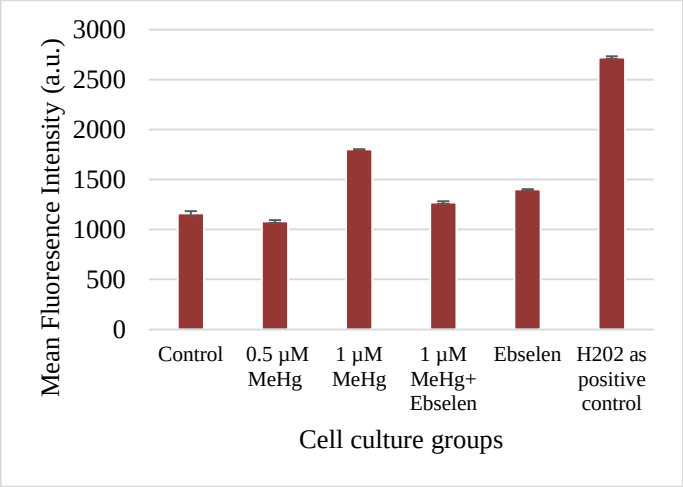

Figure-2: ROS detection by DCFDA Assay.

Scratch assay showed impaired wound closure, while invasion assay confirmed enhanced barrier disruption: The scratch assay or the wound healing assay compared cell migration rates across three conditions. In the control group, NRK52E cells exhibited robust wound closure, with cells migrating efficiently into the scratched area and significantly reducing the wound gap (Figure-3a). The cell front appeared dense, and the wound area was largely covered by newly migrated cells. Exposure to 1 µM MeHg markedly impaired wound closure. The wound gap remained wide, and the migration of cells toward the wound site was minimal. Cells near the wound edge appeared sparse, rounded, and less adherent, indicating MeHg-induced cytotoxicity and reduced migratory capacity[18] (Figure-3b). Co-treatment with 1 µM MeHg and Ebselen substantially improved wound healing compared with MeHg alone. The wound area showed partial to near-complete closure, and the migrating cell front appeared more organized and closely packed, similar to the control pattern (Figure-3c). This suggests that Ebselen restored cellular migratory ability impaired by MeHg exposure[19,20]. This assay demonstrated clear differences in cell migration among

treatment groups. Control cells displayed normal migratory behavior, consistent with healthy epithelial monolayer dynamics. MeHg-treated cells showed a pronounced defect in migration, aligning with MeHg's known effects on cytoskeletal disorganization, oxidative stress induction, and loss of cell–cell adhesion. The impaired wound closure indicates that MeHg compromises essential processes required for epithelial repair and regeneration. Ebselen co-treatment effectively counteracted these impairments. The improvement in wound closure suggests that Ebselen, through its antioxidant and glutathione peroxidase–mimetic activity, preserved cytoskeletal integrity and cell viability, thereby supporting cell motility. The enhanced cellular movement into the wound area supports findings from the Vimentin immunofluorescence results, which showed preserved cytoskeletal structure in the MeHg+Ebselen group. Overall, these results highlight Ebselen's ability to restore normal epithelial repair mechanisms disrupted by MeHg toxicity[21] (Figure-3a-c).

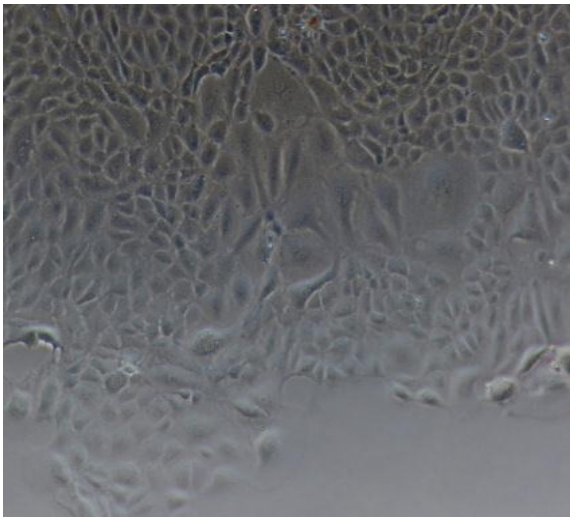

g) Control.

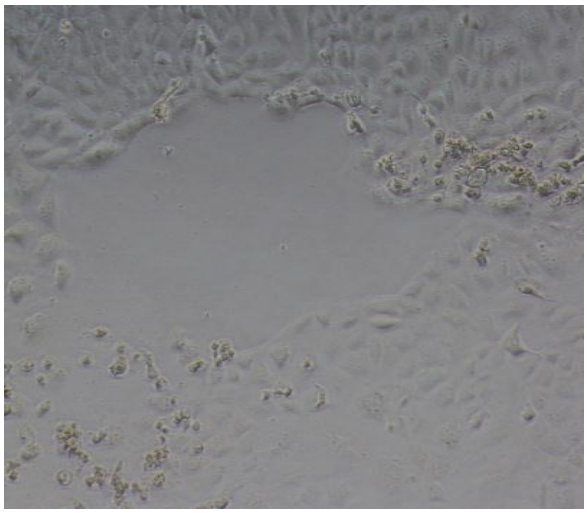

h) 1 µM MeHg.

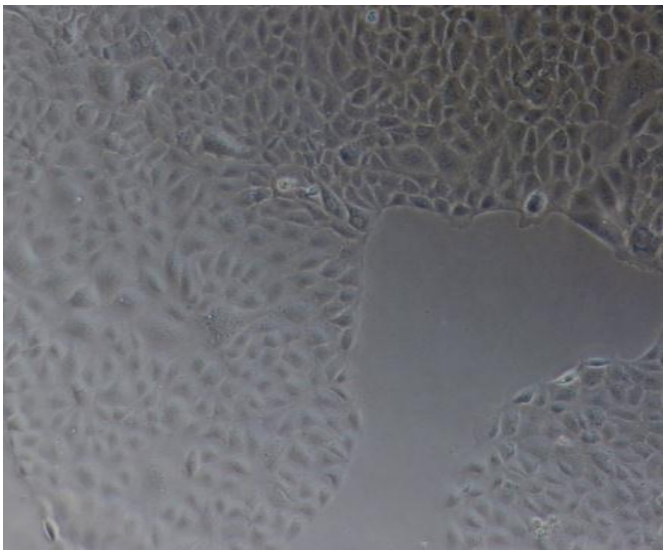

i) 1 µM MeHg + Ebselen.

Figure-3(a-c): The wound healing assay compared cell migration rates across the three conditions. The Control shows normal wound closure. The 1 µM MeHg group exhibits impaired healing, as the toxicant inhibits cell movement. In the 1 µM MeHg + Ebselen group, the Ebselen acts as an antioxidant, mitigating MeHg's damage and allowing cells to migrate and close the wound more effectively, demonstrating a rescue effect.

Invasion assay showed the effect of methylmercury (MeHg) and antioxidant treatments on cellular invasiveness. Control cells displayed normal invasion capacity, whereas MeHg treatment significantly reduced the number of invading cells, indicating impaired motility due to MeHg-induced toxicity. Co-treatment with Ebselen partially restored invasion ability nearly restoring invasion to control levels (Figure-4a-c). Data in the table represents mean number of invaded cells/fragments and highlights the protective role of Ebselen against MeHg-induced loss of cellular invasion potential (Figure-4d).

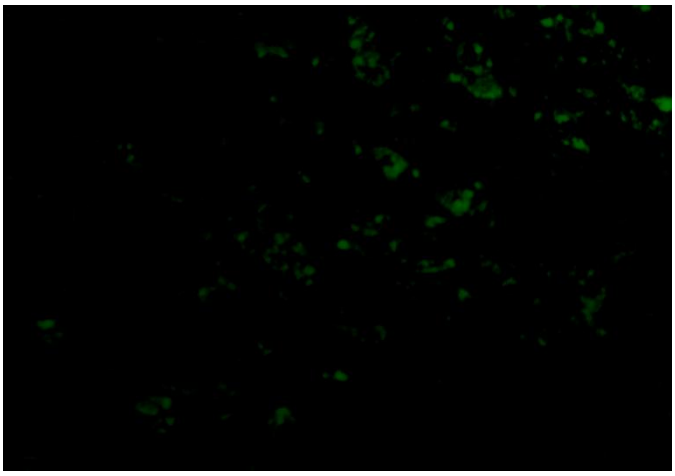

j) Control.

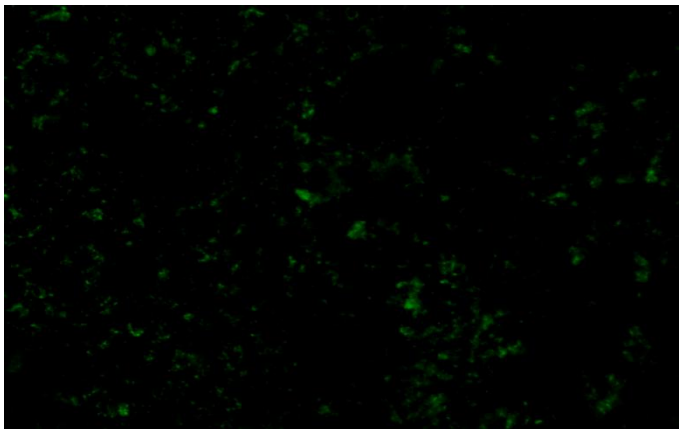

k) 1 µM MeHg.

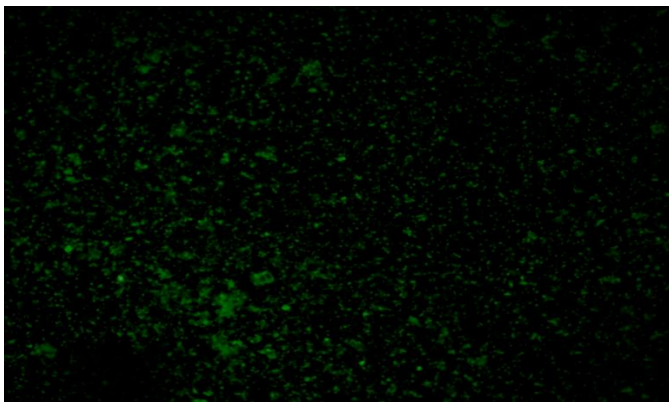

l) 1 µM MeHg + Ebselen.

Figure-4(a-c): Invasion assay showing the effect of methylmercury (MeHg) and antioxidant treatments on cellular invasiveness. Control cells displayed normal invasion capacity, whereas MeHg treatment significantly reduced the number of invading cells, indicating impaired motility due to MeHg-induced toxicity. Co-treatment with Ebselen partially restored invasion ability nearly restoring invasion to control levels. Data represent mean number of invaded cells/fragments and highlights the protective role of antioxidants against MeHg-induced loss of cellular invasion potential.

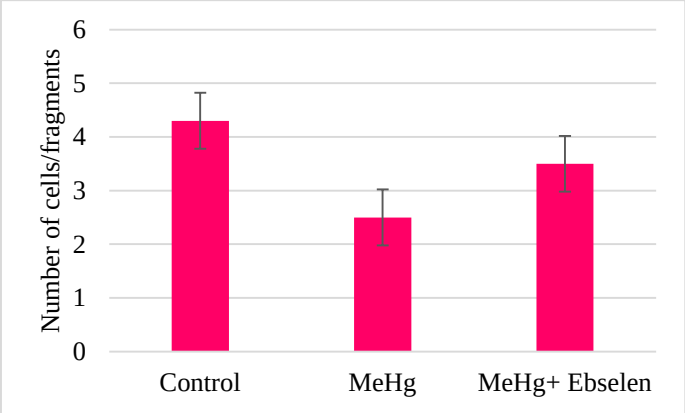

Figure-4: Invasion assay.

Abnormal levels of kidney toxicity biomarkers confirmed the cytotoxic effects of MeHg which was significantly mitigated by Ebselen co-treatment: To evaluate the protective effects of Ebselen against methylmercury (MeHg)–induced nephrotoxicity, levels of key renal injury and inflammatory biomarkers (Clusterin, MCP-1, KIM-1, IL-18, and Osteopontin) were quantified using a Luminex multiplex assay in NRK-52E cells across five treatment groups namely control, methylmercury treated, vitamin C treated, Ebselen treated and solvent control group. The assay showed that MeHg treatment significantly disrupted renal injury and inflammatory marker profiles in NRK-52E cells[22]. Clusterin levels showed a modest elevation following MeHg exposure relative to the control group, whereas Vitamin-C treatment partially attenuated this increase. In contrast, Ebselen-treated cells demonstrated clusterin levels comparable to the vehicle group, indicating minimal induction of cellular stress. A pronounced increase in MCP-1 was observed in MeHg-treated cells, confirming an inflammatory response. Vitamin-C treatment moderately reduced MCP-1, while Ebselen resulted in a marked suppression of MCP-1, restoring levels close to vehicle-treated controls. MeHg exposure also led to a substantial elevation of KIM-1, a sensitive biomarker of tubular injury. Vitamin-C further increased KIM-1 expression, whereas Ebselen dramatically lowered KIM-1 to near-baseline levels, indicating potent cytoprotective activity against MeHg-induced renal damage. IL-18 levels were markedly elevated following MeHg treatment, consistent with activation of inflammatory pathways. Ebselen significantly reduced IL-18 expression compared to both MeHg and Vitamin-C groups, while vehicle controls remained low. Osteopontin levels remained relatively unchanged in MeHg- and Vitamin-C–treated cells but were substantially decreased in the Ebselen group. This reduction further supports the anti-inflammatory and anti-injury effects of Ebselen under MeHg-induced stress. Collectively, these results demonstrate that Ebselen robustly attenuates MeHg-induced renal injury and inflammation in NRK-52E cells, as evidenced by the normalization of multiple biomarkers associated with nephrotoxicity. Ebselen consistently outperformed Vitamin-C across all measured parameters, highlighting its therapeutic potential in mitigating mercury-induced cellular damage[23] (Figure-5).

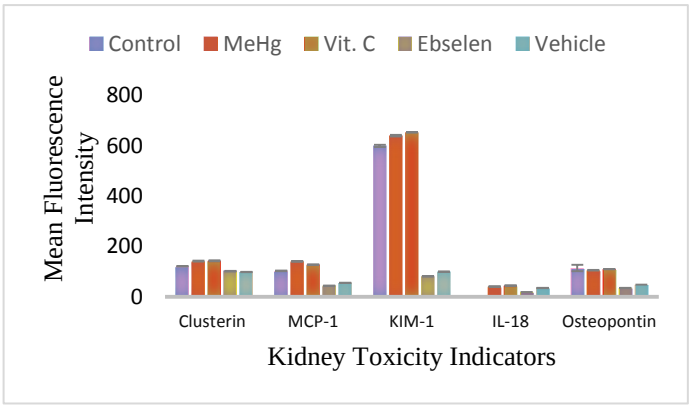

Figure-5: Kidney Toxicity Indicators.

E-cadherin down regulation and vimentin upregulation indicated EMT induction, confirming cytoskeletal reorganization and disassembly of cell junctions: To determine whether MeHg induces epithelial–mesenchymal transition (EMT) in NRK-52E cells and whether Ebselen attenuates this response, E-cadherin localization using immunofluorescence was accessed (Figure-6a-c)).

Under control conditions (Figure-6a), cells displayed strong, continuous membrane-associated E-cadherin, with clear cell–cell border definition and a uniform epithelial monolayer. The red fluorescence showed tight functional organization characteristic of an intact epithelial phenotype.

Exposure to 1 µM MeHg caused a pronounced decrease in E-cadherin signal intensity and disrupted its membrane localization (Figure 6b)[24,25].

The fluorescence distribution became diffuse and more cytoplasmic, and cell–cell junctions appeared irregular and weakened. The epithelial sheet showed areas of discontinuity and morphological disorganization, consistent with early EMT-like structural changes[26]. Co-treatment of 1 µM MeHg with Ebselen partially restored E-cadherin expression (Figure-6c).

Although the intensity did not reach control levels, the membrane-associated signal became more continuous, and intercellular borders were visibly better preserved compared with MeHg alone. Cell morphology appeared more compact and cohesive, reflecting a re-establishment of epithelial junction integrity.

These results demonstrate that MeHg exposure reduces epithelial integrity in NRK-52E cells by suppressing membrane-localized E-cadherin—a hallmark event in EMT initiation. The loss of adherens junction structure and the shift toward diffuse, cytoplasmic staining patterns observed after 1 µM MeHg treatment are consistent with EMT-associated remodeling, wherein cells lose polarity and intercellular adhesion.

These observations align with established mechanisms in which heavy metal-induced oxidative stress activates EMT-driving transcription factors such as Snail, Twist, and ZEB families, ultimately repressing E-cadherin expression. Ebselen co-treatment attenuated these MeHg-induced alterations, as evidenced by the improved continuity of E-cadherin staining along cell borders.

This protective effect is consistent with Ebselen's known antioxidant and glutathione-peroxidase–mimetic properties, which can reduce intracellular oxidative burden and interfere with redox-sensitive signaling pathways that regulate EMT. Although the rescue was partial, the restoration of junctional localization suggests that Ebselen helps preserve epithelial phenotype under chemical stress[27].

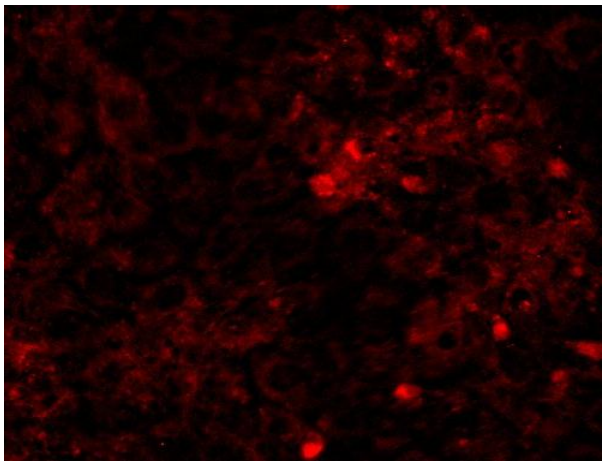

m (i).

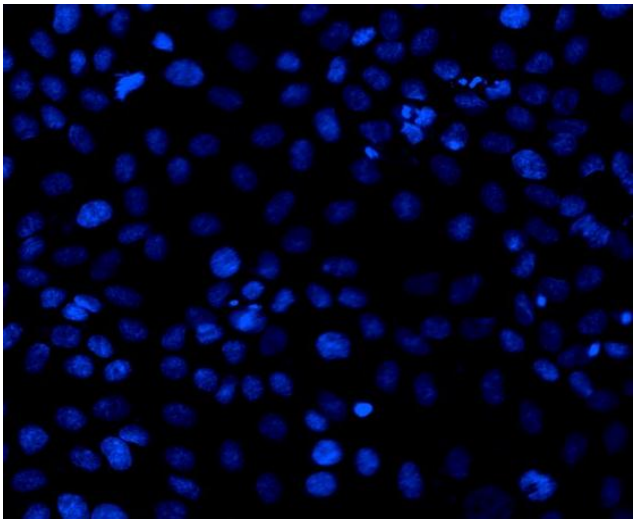

a (ii)

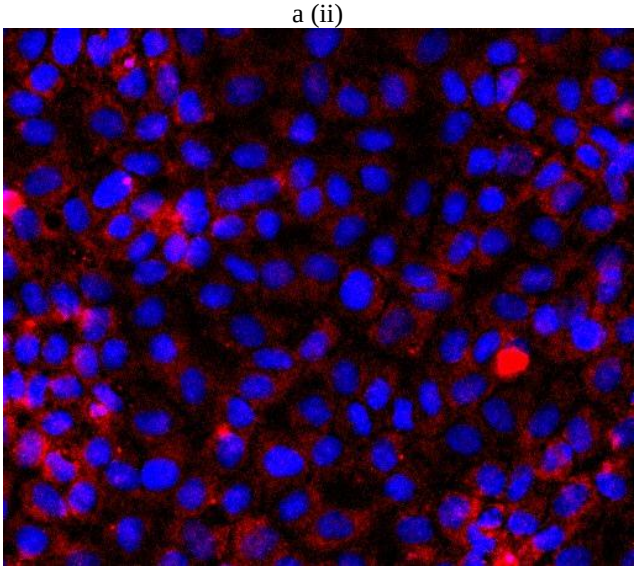

a (iii)

Figure-6a (i-iii) Control: Cells exhibit strong, continuous membrane-localized E-cadherin, forming a compact epithelial monolayer with well-defined cell borders.

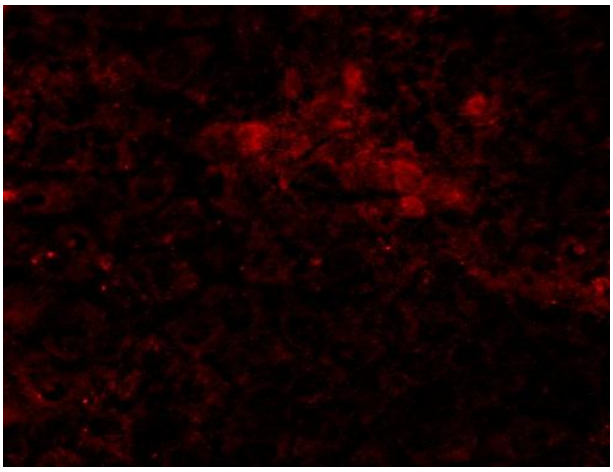

b (i)

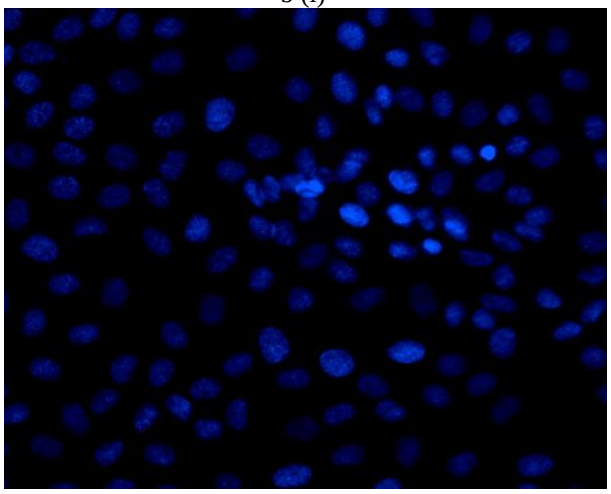

b (ii)

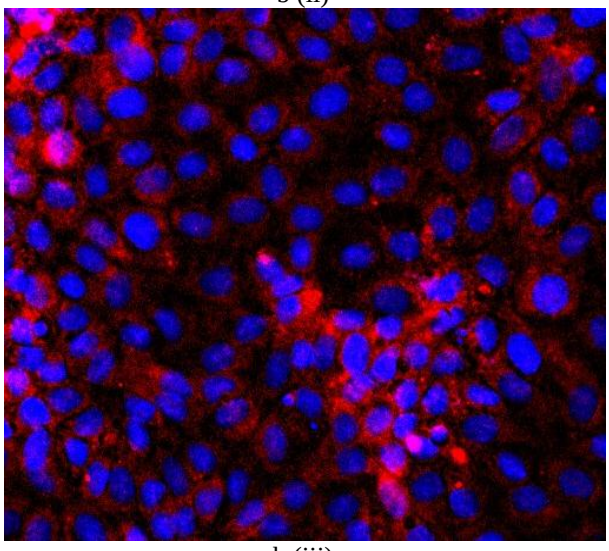

b (iii)

Figure-6b (i-iii) 1 µM MeHg: MeHg exposure markedly reduces E-cadherin intensity and disrupts its membrane distribution, resulting in diffuse cytoplasmic staining and loss of epithelial junctional integrity, indicative of EMT-like changes.

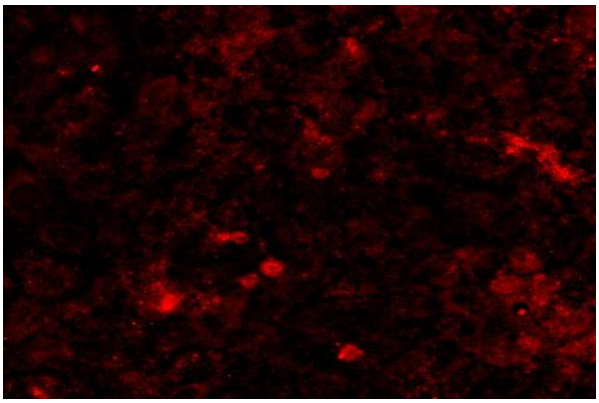

c (i)

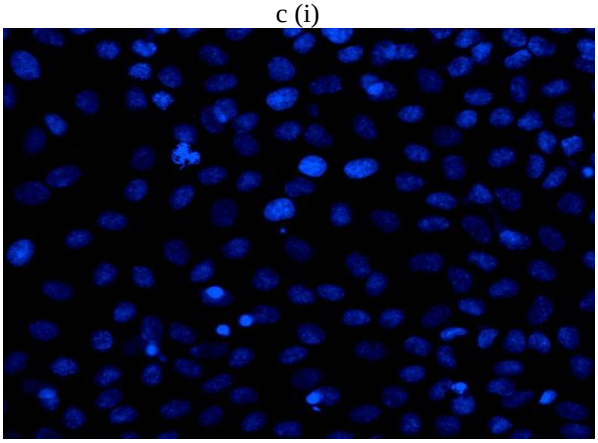

c (ii)

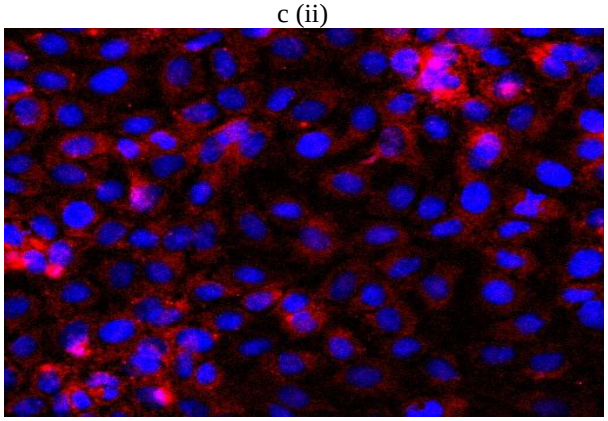

c (iii)

Figure-6c (i-iii) 1 µM MeHg + Ebselen: Co-treatment with Ebselen partially restores membrane-associated E-cadherin and improves cell–cell junction continuity compared with MeHg alone, reflecting attenuation of MeHg-induced EMT.

Figure-6: Effects of MeHg and Ebselen on E-cadherin expression in NRK-52E cells.

Representative immunofluorescence images showing E-cadherin in the cell monolayer (red), nuclear staining with DAPI (blue) and merged (red and blue) under (a) Control, (b) 1 µM MeHg, and (c) 1 µM MeHg + 10 µM Ebselen conditions.

Figure-6: a (i-iii) Control: Cells exhibit strong, continuous membrane-localized E-cadherin, forming a compact epithelial monolayer with well-defined cell borders.

Figure-6b (i-iii) 1 µM MeHg: MeHg exposure markedly reduces E-cadherin intensity and disrupts its membrane distribution, resulting in diffuse cytoplasmic staining and loss of epithelial junctional integrity, indicative of EMT-like changes.
Figure-6c (i-iii) 1 µM MeHg + Ebselen: Co-treatment with Ebselen partially restores membrane-associated E-cadherin and improves cell–cell junction continuity compared with MeHg alone, reflecting attenuation of MeHg-induced EMT.

Immunofluorescence analysis of Vimentin revealed distinct differences among the control, MeHg-treated, and MeHg+Ebselen treated NRK52E cells (Figure-7a-c). In the control group (Figure-7a), cells showed strong Vimentin expression with a well-organized filamentous cytoplasmic network, accompanied by uniformly shaped and clearly defined nuclei. Exposure to 1 µM MeHg (Figure-7b) resulted in a marked reduction in Vimentin fluorescence intensity, with the cytoskeletal filaments appearing diffuse and disorganized[28]. Subtle nuclear irregularities were observed, suggesting early cellular stress. In contrast, cells co-treated with 1 µM MeHg and Ebselen (Figure-7c) exhibited restored Vimentin expression, with filament organization resembling that of the control group. Nuclear morphology also appeared preserved, indicating a protective effect of Ebselen. The strong and organized Vimentin network observed in untreated NRK52E cells reflects a healthy cytoskeletal architecture essential for maintaining epithelial structure, stability, and function. MeHg exposure disrupted this organization, consistent with its known cytotoxic effects mediated through oxidative stress, protein dysfunction, and destabilization of intermediate filaments. The weakened and diffuse Vimentin pattern suggests early cytoskeletal collapse, which may contribute to EMT-like changes or increased cellular susceptibility to damage. Co-treatment with Ebselen markedly reversed MeHg-induced cytoskeletal alterations. Ebselen's antioxidant and glutathione peroxidase–mimetic properties likely counteracted MeHg-mediated ROS generation, thereby preserving Vimentin structure and protecting cellular integrity. The recovery of Vimentin filament organization and the maintenance of normal nuclear morphology support Ebselen's role as a potent cytoprotective agent[29].

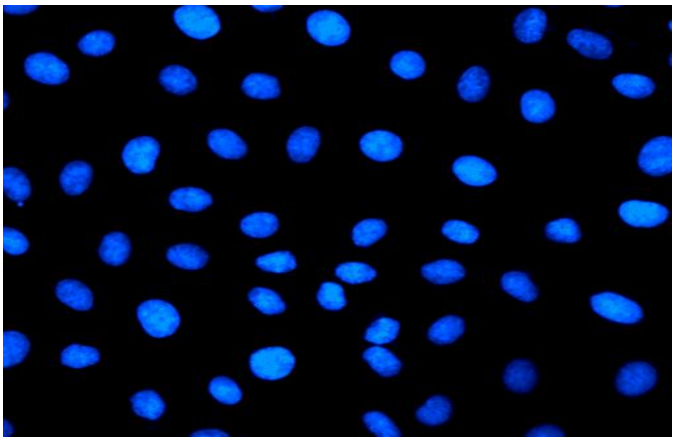

a (ii).

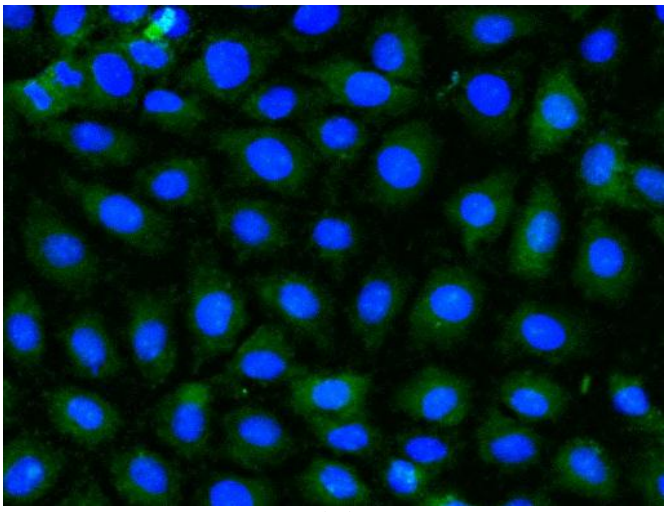

a (iii).

Figure-7a (i-iii) Control: Cells exhibited strong Vimentin expression with a well-organized filamentous cytoplasmic network and uniformly shaped nuclei, indicating intact cytoskeletal structure.

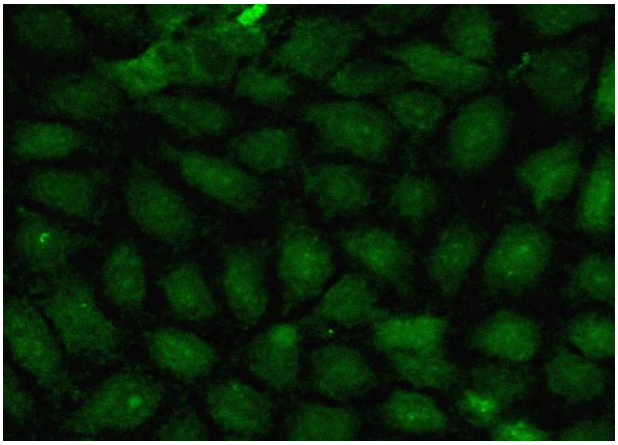

n (i).

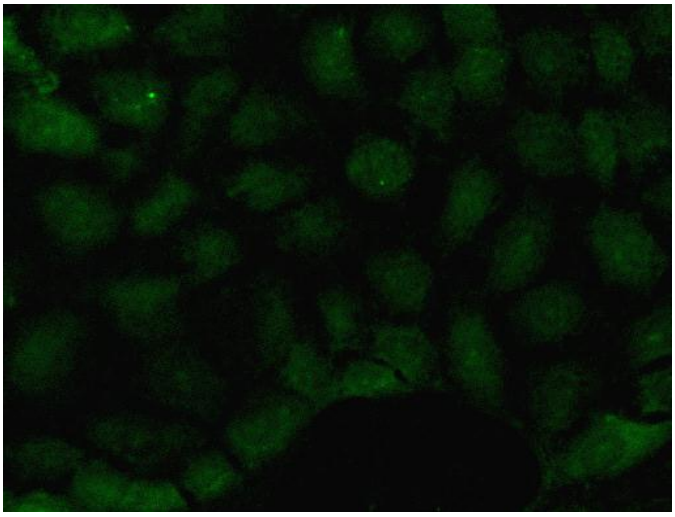

b (i).

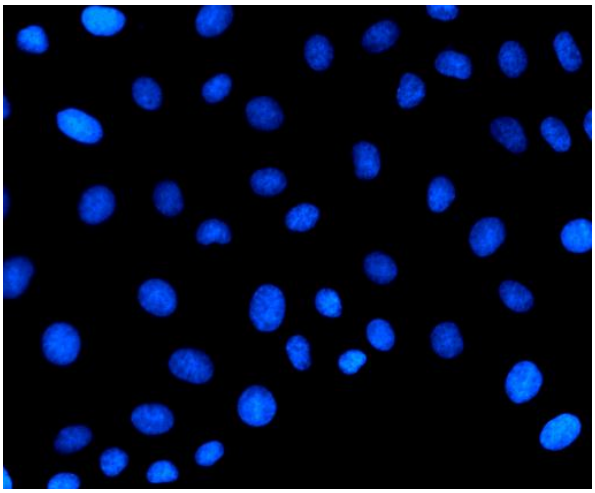

o (ii).

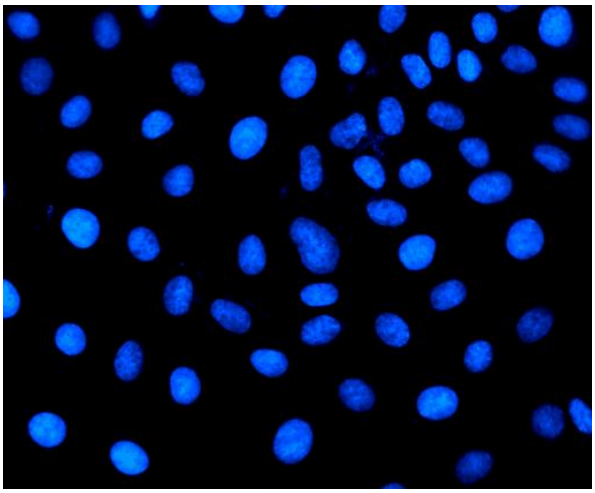

c (ii).

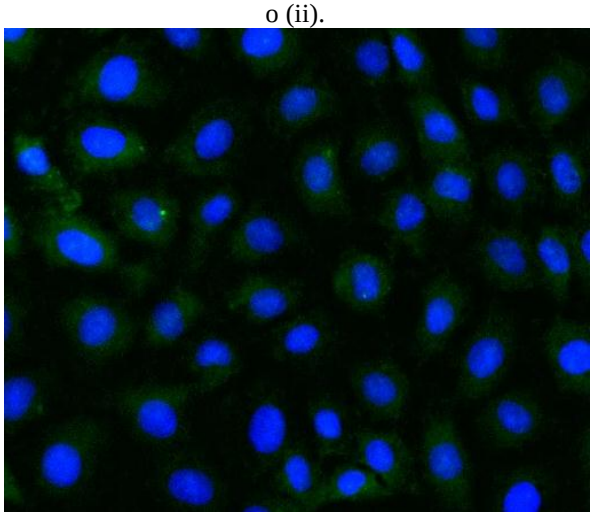

p (iii).

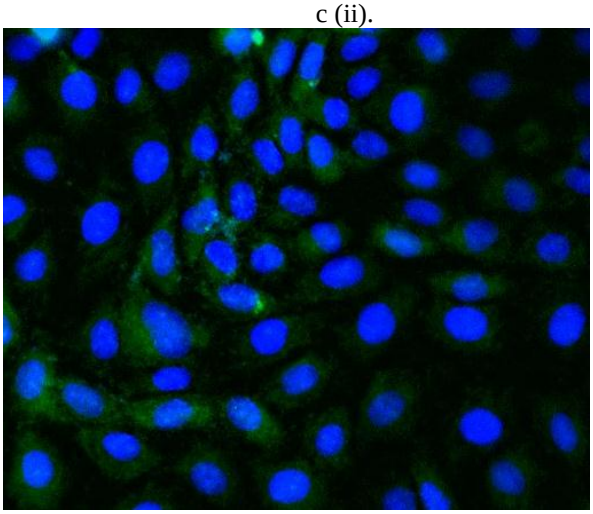

q (iii).

Figure-7b (i-iii) 1 µM MeHg : Cells treated with 1 µM MeHg showed reduced Vimentin fluorescence intensity with a diffuse and disorganized filament pattern, along with subtle nuclear irregularities, suggesting early cytoskeletal disruption and cellular stress.

Figure-7c (i-iii) 1 µM MeHg + Ebselen: Co-treatment with 1 µM MeHg and Ebselen restored Vimentin expression and filament organization, displaying a pattern comparable to control cells. Nuclear morphology also remained intact, demonstrating the protective effect of Ebselen against MeHg-induced cytoskeletal alterations.

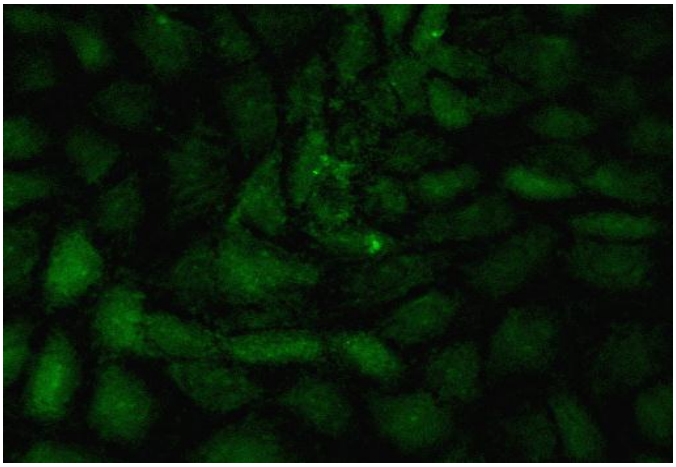

c (i).

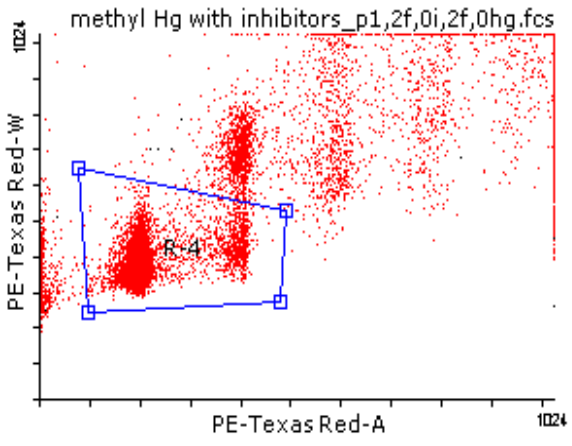

r (i).

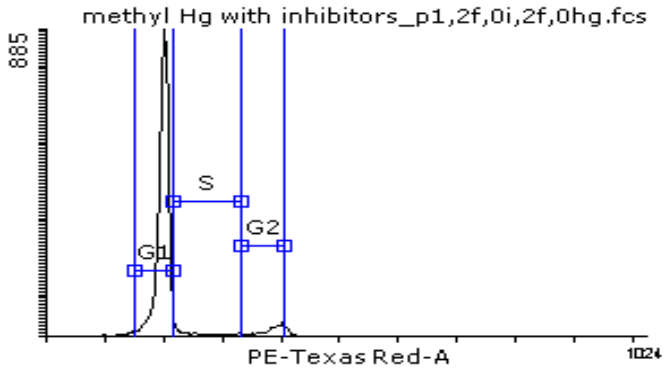

a (ii).

	Events	% of Vis	Mean	GeoMean	Media
All events	9,412	100.00	214.23	209.23	201.0
G1	8,110	86.17	197.85	197.57	200.0
G2	549	5.83	382.97	382.51	388.0
S	457	4.86	259.01	256.55	250.0

a (iii).

Figure-8(a): Flow-cytometric assessment of cell-cycle distribution in NRK52E cells exposed to methylmercury with inhibitor p1, 2f, 0i, 2f, 0hg.fcs. (i) Dot-plot of PE–Texas Red-A versus PE–Texas Red-W showing the gating strategy used to isolate single-cell events. The polygon gate (blue) excludes debris, doublets, and aggregates, ensuring accurate identification of true single cells for downstream analysis. (ii) Histogram of DNA content (PE–Texas Red-A) depicting the distribution of NRK52E cells across the G1, S, and G2 phases following methylmercury exposure in the presence of inhibitors. Peaks corresponding to each phase are annotated, illustrating treatment-induced shifts in cell-cycle progression. (iii) Representative table shows the distribution of cellular events across different phases of the cell cycle under. A total of 9,412 events were analyzed, with the majority of cells residing in the G1 phase (86.17%), followed by G2 phase (5.83%) and S phase (4.86%). The table displays the Mean, GeoMean, Median, and Coefficient of Variation (CV) for fluorescence intensity values corresponding to each cell-cycle phase. These parameters reflect the cellular DNA content and indicate phase-specific population dynamics essential for assessing treatment-induced alterations in cell-cycle progression.

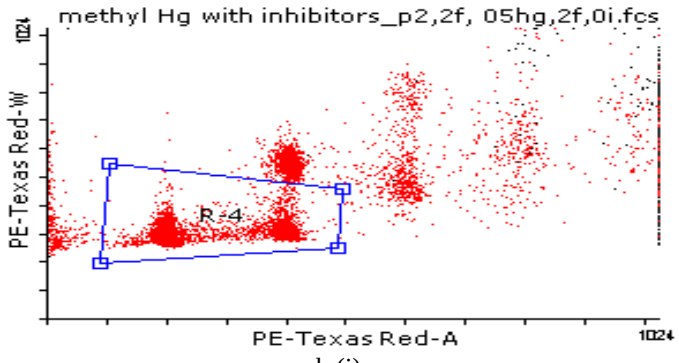

b (i).

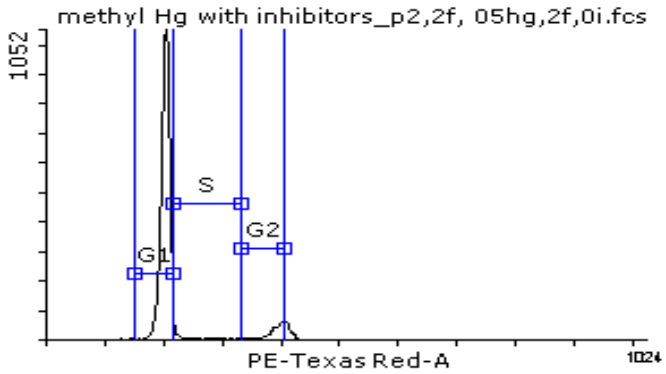

b (ii).

	Events	% of Vis	Mean	GeoMean	Median	CV
All events	10,092	100.00	225.89	219.41	204.00	28.04
G1	8,487	84.10	202.06	201.91	203.00	3.78
G2	752	7.45	385.48	385.04	391.00	4.70
S	397	3.93	253.84	251.48	242.00	13.97

s (iii).

Figure-8(b): Flow-cytometric evaluation of cell-cycle distribution in NRK52E cells exposed to methylmercury in the presence of inhibitors (p2,2f,05hg,2f,0i.fcs). (i) Representative dot-plot illustrating the gating strategy used to isolate singlet NRK52E cell populations for analysis. The R4 gate was drawn based on PE-Texas Red-A versus PE-Texas Red-W parameters to effectively exclude debris, dead cells, aggregates, and doublets, ensuring accurate assessment of DNA content and cell-cycle progression. (ii) DNA content histogram depicting cell-cycle phase distribution (G1, S, and G2/M phases) in methylmercury-treated cells co-exposed to inhibitors. Distinct peaks corresponding to G1, S, and G2/M populations are clearly separated, allowing precise quantification of cell-cycle arrest or progression upon treatment. (iii) Summary table of flow-cytometry-derived cell-cycle parameters, including total events analyzed, percentage of cells in each phase (G1, S, and G2/M), and statistical descriptors (Mean, GeoMean, Median, CV). The results reveal a dominant G1 population (84.10%), a reduced S-phase fraction (3.93%), and a moderate G2/M population (7.45%), indicating that methylmercury exposure in the presence of inhibitors predominantly restricts cells at the G1 phase while limiting progression into S and G2/M phases. These findings suggest that the inhibitor treatment modulates MeHg-induced cell-cycle dysregulation.

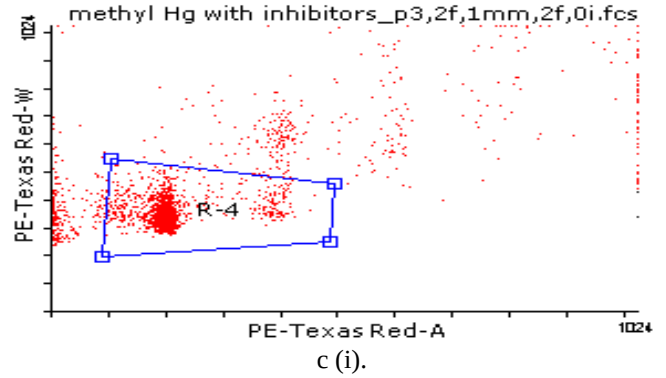

c (i).

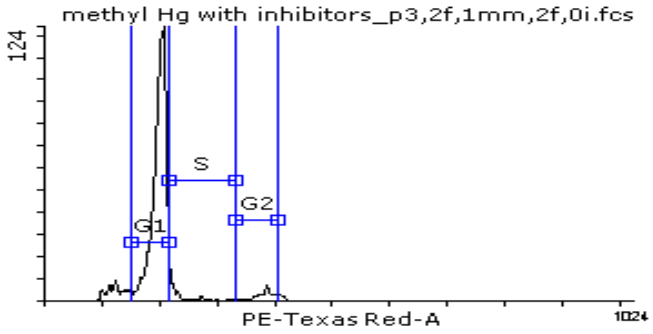

c (ii).

	Events	% of Vis	Mean	GeoMean	Median	CV
All events	1,741	100.00	206.61	200.91	201.00	26.09
G1	1,396	80.18	197.76	197.38	200.00	6.04
G2	85	4.88	380.93	380.54	384.00	4.43
S	107	6.15	244.85	242.82	230.00	13.51

t (iii).

Figure-8(c): Cell-cycle profile of NRK52E cells treated with methylmercury in the presence of inhibitors (p3, 2f, 1mm, 2f, 0i). (i) Dot-plot showing the gating strategy used to isolate the R4 population for cell-cycle analysis. The PE-Texas Red-A vs. PE-Texas Red-W plot was used to exclude debris, dead cells, and doublets, ensuring accurate quantification of DNA content in single-cell events. (ii) DNA content histogram illustrating the distribution of NRK52E cells across the G1, S, and G2/M phases following exposure to methylmercury with inhibitors. Distinct peaks corresponding to G1, S, and G2/M populations are marked, enabling precise assessment of treatment-related shifts in cell-cycle progression. (iii) Summary table depicting numerical flow-cytometric data, including total events, percentage of cells in each cell-cycle phase, and statistical parameters (Mean, GeoMean, Median, CV). The results indicate that 80.18% of cells remained in the G1 phase, while 6.15% and 4.88% were distributed in the S and G2 phases, respectively. This pattern suggests that the inhibitor combination partially mitigates methylmercury-induced cell-cycle disruption, maintaining a predominantly G1-phase population with limited progression into S and G2/M.

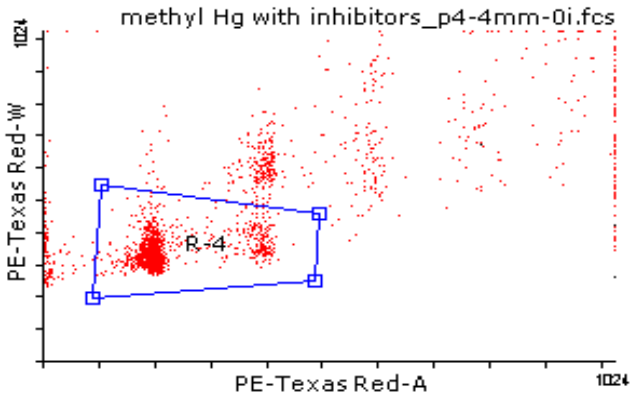

d (i).

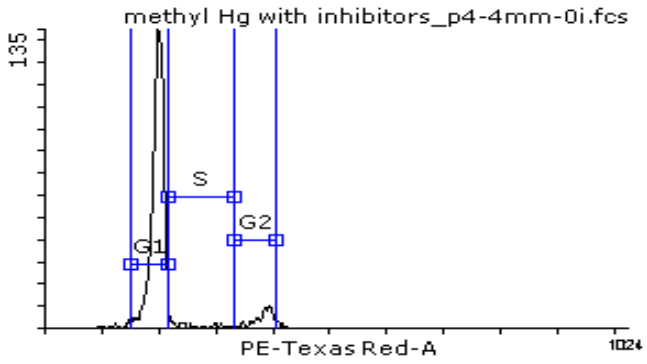

d (ii).

	Events	% of Vis	Mean	GeoMean	Median	CV
All events	1,779	100.00	215.37	209.45	200.00	27.13
G1	1,502	84.43	196.46	196.13	199.00	5.60
G2	145	8.15	382.23	381.85	386.00	4.37
S	78	4.38	263.28	260.63	254.00	14.38

d (iii).

Figure-8(d): Cell-cycle distribution of NRK52E cells exposed to methylmercury with inhibitor combination p4–4 mm–0i. (i) Dot-plot showing the gating strategy applied to identify the R4 singlet cell population for cell-cycle assessment. The PE-Texas Red-A versus PE-Texas Red-W scatter plot was used to exclude debris, dead cells, and doublets, ensuring accurate DNA-content measurement. (ii) Representative DNA-content histogram depicting the distribution of NRK52E cells across the G1, S, and G2/M phases following treatment with methylmercury in the presence of the p4 inhibitor combination. Peaks corresponding to G1, S, and G2/M phases are clearly marked, enabling quantification of treatment-related alterations in cell-cycle progression. (iii) Flow-cytometric summary table showing total events, percentage of cells in each cell-cycle phase, and statistical parameters (Mean, Geomean, Median, and CV). The analysis reveals that 84.43% of cells remained in G1 phase, while 4.38% and 8.15% were distributed in S and G2 phases, respectively. This distribution suggests a predominant G1-phase retention with limited progression into S and moderate G2 accumulation, indicating partial modulation of methylmercury-induced cell-cycle dysregulation by the inhibitor combination.

Cell-cycle machinery remains significantly impaired even when MeHg toxicity is partially suppressed by Ebselen cotreatment: Flow cytometric analysis of NRK52E cells revealed distinct alterations in the distribution of cell populations across different phases of the cell cycle under MeHg and Ebselen treatments. Flow-cytometric analysis (Figure-8a-d) showed that methylmercury (MeHg) exposure induced marked alterations in the cell-cycle distribution of NRK-52E cells[30]. In Figure-8a, representing the MeHg condition with baseline inhibitor mixture, a prominent accumulation of cells in the G1 phase was observed, accompanied by a substantial reduction in the S-phase population and a small G2/M fraction. This shift suggested that MeHg primarily triggered G1-phase arrest, restricting DNA synthesis and progression into S phase. In Figure-8b, MeHg

with the p2-2f inhibitor combination exhibited a similar dispersed pattern in the dot plot, with a tight gated cluster (R4), indicating the presence of a stressed or growth-restricted cell population. The fluorescence intensity suggested partial recovery, but the S-phase population remained low, consistent with continued suppression of DNA synthesis. Fig. 8c, representing MeHg + p4-4mM inhibitor, showed a comparable tight gating region with a modestly more dispersed distribution, indicating that although the inhibitor slightly improved cell-cycle uniformity, the overall pattern remained indicative of MeHg-induced stress. The distribution again suggested persistence of G1 accumulation with limited S-phase restoration. In Fig. 8d, the MeHg + p4-4mM–0i condition exhibited similar gating characteristics, with a high density of events in the lower region, reflecting a predominantly G1-rich population. No substantial shift toward S or G2/M phases was visible, confirming that even with modified inhibitor combinations, MeHg continued to restrict normal cell-cycle progression. These results demonstrate that MeHg treatment consistently suppresses S-phase entry and maintains cells in G1 arrest across all tested inhibitor conditions, with only minor variations in the degree of distribution broadening.

It clearly indicates that methylmercury is a potent inducer of G1-phase arrest in NRK-52E cells, significantly impairing their ability to progress through the cell cycle[31]. This is consistent with MeHg's known capacity to cause oxidative stress, mitochondrial dysfunction, DNA damage, and disruption of essential cell-cycle regulators such as cyclins and CDKs. The pronounced reduction in S-phase cells across all conditions reflects inhibition of DNA synthesis, a common hallmark of toxic heavy metals that limit nucleotide incorporation and DNA replication machinery efficiency. The relatively small G2/M fraction across all figures further confirms that few cells were able to complete S phase and advance to mitosis. Two inhibitor combinations suggested slightly improved clustering; none of the inhibitor treatments restored a normal distribution of S-phase events. This indicates that MeHg-induced G1 arrest is dominant and difficult to reverse, Ebselen mitigated oxidative stress but did not fully restore DNA replication, and C\cell-cycle machinery remained significantly impaired even when MeHg toxicity was partially suppressed.

Conclusion

The findings of this study collectively demonstrate the strong therapeutic potential of Ebselen in counteracting mercury-induced renal cell injury and promoting functional wound repair. Methylmercury exposure disrupted epithelial homeostasis in NRK52E cells, as evidenced by increased cytotoxicity markers, loss of membrane integrity, and pronounced morphological deterioration[32]. This damage was accompanied by classical features of epithelial–mesenchymal transition (EMT), including down regulation of E-cadherin and upregulation of vimentin, indicating a shift toward a mesenchymal, migratory, and injury-prone phenotype. Ebselen significantly ameliorated these pathological alterations. Restoration of E-cadherin expression and suppression of vimentin over expression highlight its role in reversing or preventing MeHg-induced EMT. Moreover, cell-cycle profiling revealed that methylmercury caused an arrest in key regulatory phases associated with DNA damage and stress response, whereas Ebselen co-treatment normalized cell-cycle distribution, suggesting improved cellular recovery and reduced genotoxic burden. Functional assays further strengthened these observations. In the wound-healing assay, Ebselen markedly improved cell migration rates, facilitating more efficient closure of MeHg-induced gaps and promoting tissue repair. Similarly, in the invasion assay, Ebselen mitigated the aberrant, injury-associated invasive behavior triggered by methylmercury, indicating a restoration of controlled epithelial dynamics rather than pathological motility[33]. Its impact on cytotoxicity markers, including reduced ROS levels and preserved viability, underscores its antioxidant and cytoprotective capabilities. Ebselen demonstrates a multifaceted protective effect by reducing cytotoxicity, restoring epithelial markers, normalizing cell-cycle progression, and enhancing wound repair while controlling aberrant invasion. These integrated outcomes strongly support Ebselen as a promising therapeutic candidate for mitigating mercury-induced nephrotoxicity and promoting renal epithelial repair. Further in-vivo exploration and mechanistic studies could strengthen its development as a clinically relevant protective agent.

Acknowledgement

We sincerely express our gratitude to Prof. D.C. Rai, Hon'ble Vice-Chancellor of B.R.A. Bihar University, Muzaffarpur, and the Prof. Ravindra Kumar Chaudhary, Principal of MJK College, Bettiah, for their unwavering support and encouragement. We extend our heartfelt thanks to Dr. Rakesh Mohan Rai, Head of the University PG Department of Zoology, and Dr. H. Khan, my Ph.D. guide and co-author of this research paper, for their continuous guidance and academic mentorship.

We are especially thankful to Department of Zoology and Biotechnology, Mahatma Gandhi Central University, Motihari for providing essential laboratory facilities and valuable technical assistance that were crucial to the successful execution of this research.

References

1. Ke, T., Gonçalves, F. M., Gonçalves, C. L., Dos Santos, A. A., Rocha, J. B. T., Farina, M., Skalny, A., Tsatsakis, A., Bowman, A. B., & Aschner, M. (2019). Post-translational modifications in MeHg-induced neurotoxicity. *Biochimica et biophysica acta*. Molecular basis of disease, 1865(8), 2068–2081. https://doi.org/10.1016/j.bbadis.2018.10.024

2. Branco, V., Coppo, L., Solá, S., Lu, J., Rodrigues, C. M. P., Holmgren, A., & Carvalho, C. (2017). Impaired cross-talk between the thioredoxin and glutathione systems is related

to ASK-1 mediated apoptosis in neuronal cells exposed to mercury. *Redox Biology*, 13, 278–287. https://doi.org/10.1016/j.redox.2017.05.024

3. Farina, M., Aschner, M., & Rocha, J. B. (2011). Oxidative stress in MeHg-induced neurotoxicity. *Toxicology and applied pharmacology*, 256(3), 405–417. https://doi.org/10.1016/j.taap.2011.05.001

4. Genchi, G., Sinicropi, M. S., Lauria, G., Carocci, A., & Catalano, A. (2020). The Effects of Cadmium Toxicity. *International journal of environmental research and public health*, 17(11), 3782. https://doi.org/10.3390/ijerph17113782

5. Lu, Q., Cai, Y., Xiang, C., Wu, T., Zhao, Y., Wang, J., … Zou, L. (2021). Ebselen, a multi-target compound: its effects on biological processes and diseases. *Expert Reviews in Molecular Medicine*, 23, e12. doi:10.1017/erm.2021.14

6. Amporndanai, K., Meng, X., Shang, W. et al. (2021). Inhibition mechanism of SARS-CoV-2 main protease by ebselen and its derivatives. *Nat Commun*, 12, 3061 (2021). https://doi.org/10.1038/s41467-021-23313-7

7. Miyano, T., Suzuki, A., & Sakamoto, N. (2021). Hyperosmotic stress induces epithelial-mesenchymal transition through rearrangements of focal adhesions in tubular epithelial cells. *PLoS One*, 16(12), e0261345.

8. Karaboga, Ihsan & Okuyan, Hamza Malik & Doğan, Serdar & Ayçiçek, Şeyda & Çakıroğlu, Hüseyin. (2025). Ebselen Alleviates Sepsis- Induced Acute Kidney Injury by Regulating Endoplasmic Reticulum Stress, Apoptosis, and Oxidative Stress. *Veterinary Medicine and Science*, 11. 10.1002/vms3.70318.

9. Han, B., Lv, Z., Han, X., Li, S., Han, B., Yang, Q., Wang, X., Wu, P., Li, J., Deng, N., & Zhang, Z. (2022). Harmful Effects of Inorganic Mercury Exposure on Kidney Cells: Mitochondrial Dynamics Disorder and Excessive Oxidative Stress. *Biological trace element research*, 200(4), 1591–1597. https://doi.org/10.1007/s12011-021-02766-3

10. Azad, G. K., & Tomar, R. S. (2014). Ebselen, a promising antioxidant drug: mechanisms of action and targets of biological pathways. *Molecular biology reports*, 41(8), 4865–4879. https://doi.org/10.1007/s11033-014-3417-x

11. Ransy, C., Vaz, C., Lombès, A., & Bouillaud, F. (2020). Use of H_2O_2 to Cause Oxidative Stress, the Catalase Issue. *International journal of molecular sciences*, 21(23), 9149. https://doi.org/10.3390/ijms21239149

12. Xiaoyang Li, Jingjing Pan, Yanfeng Wei, Linlin Ni, Bin Xu, Yu Deng, Tianyao Yang, Wei Liu, (2021). Mechanisms of oxidative stress in methylmercury-induced neurodevelopmental toxicity. *Neuro Toxicology*, 85, 33-46. https://doi.org/10.1016/j.neuro.2021.05.002

13. Verma, S., Singh, P., Khurana, S., Ganguly, N. K., Kukreti, R., Saso, L., Rana, D. S., Taneja, V., & Bhargava, V. (2021). Implications of oxidative stress in chronic kidney disease: a review on current concepts and therapies. *Kidney research and clinical practice*, 40(2), 183–193. https://doi.org/10.23876/j.krcp.20.163

14. Yao, D., et al. (2023). Molecular insights into methylmercury-induced redox imbalance and protective role of antioxidants. *Free Radical Biology and Medicine*, 201, 123–133.

15. Abdelazim, A. M., & Abomughaid, M. M. (2024). Oxidative stress: an overview of past research and future insights. *All Life*, 17(1). https://doi.org/10.1080/26895293.2024.2316092

16. Perez-Araluce, M., Jüngst, T., Sanmartin, C., Prosper, F., Plano, D., & Mazo, M. M. (2024). Biomaterials-Based Antioxidant Strategies for the Treatment of Oxidative Stress Diseases. *Biomimetics*, 9(1), 23.

17. Muscolo, A., Mariateresa, O., Giulio, T., & Mariateresa, R. (2024). Oxidative Stress: The Role of Antioxidant Phytochemicals in the Prevention and Treatment of Diseases. *International journal of molecular sciences*, 25(6), 3264. https://doi.org/10.3390/ijms25063264

18. Farina, M., Rocha, J. B. T., & Aschner, M. (2011). Mechanisms of methylmercury-induced neurotoxicity: Evidence from experimental studies. *Life Sciences*, 89(15 16), 555–563.

19. Yoon, Y., Kim, Y., Kim, S. Y., et al. (2013). Ebselen attenuates renal ischemia-reperfusion injury in rats. *American Journal of Physiology-Renal Physiology*, 304(8), F919–F927.

20. Kurauchi, Y., et al. (2022). Protective effect of Ebselen on cisplatin-induced kidney injury through Nrf2 pathway activation. *Toxicology and Applied Pharmacology*, 449, 116105. https://doi.org/10.1016/j.taap.2022.116105

21. Lu, Q., Cai, Y., Xiang, C., Wu, T., Zhao, Y., Wang, J., … Zou, L. (2021). Ebselen, a multi-target compound: its effects on biological processes and diseases. *Expert Reviews in Molecular Medicine*, 23, e12. doi:10.1017/erm.2021.14

22. Vaidya, V. S., Ferguson, M. A., & Bonventre, J. V. (2010). Biomarkers of acute kidney injury. *Annual Review of Pharmacology and Toxicology*, 48, 463–493.

23. Ghosh, R., et al. (2022). Antioxidant-based strategies for combating heavy metal toxicity: focus on selenium compounds. *Antioxidants*, 11(9), 1702. https://doi.org/10.3390/antiox11091702

24. Kaur, G., et al. (2021). Oxidative stress and methylmercury nephrotoxicity: emerging insights into molecular mechanisms. *Journal of Applied Toxicology*, 41(4), 552 563. https://doi.org/10.1002/jat.4091

25. Li, B., Qiao, C., Jin, X., & Chan, H. M. (2021). Characterizing the Low-Dose Effects of Methylmercury on the Early Stages of Embryo Development Using Cultured Human Embryonic Stem Cells. *Environmental health perspectives*, 129(7), 77007. https://doi.org/10.1289/EHP7349

26. Jomova, K., Alomar, S. Y., Nepovimova, E., Kuca, K., & Valko, M. (2025). Heavy metals: toxicity and human health effects. *Archives of toxicology*, 99(1), 153–209. https://doi.org/10.1007/s00204-024-03903-2

27. Yao, D., et al. (2023). Molecular insights into methylmercury-induced redox imbalance and protective role of antioxidants. *Free Radical Biology and Medicine*, 201, 123–133.

28. Navas, T., Kinders, R. J., Lawrence, S. M., Ferry-Galow, K. V., Borgel, S., Hollingshead, M. G., Srivastava, A. K., Alcoser, S. Y., Makhlouf, H. R., Chuaqui, R., Wilsker, D. F., Konaté, M. M., Miller, S. B., Voth, A. R., Chen, L., Vilimas, T., Subramanian, J., Rubinstein, L., Kummar, S., Chen, A. P., … Parchment, R. E. (2020). Clinical Evolution of Epithelial-Mesenchymal Transition in Human Carcinomas. *Cancer research*, 80(2), 304–318. https://doi.org/10.1158/0008-5472.CAN-18-3539

29. Zhao, X., et al. (2023). Ebselen as a therapeutic antioxidant: advances and challenges. *Redox Biology*, 58, 102568. https://doi.org/10.1016/j.redox.2023.102568

30. Zhu, X., Kusaka, Y., Sato, K., & Zhang, Q. (2000). The endocrine disruptive effects of mercury. *Environmental health and preventive medicine*, 4(4), 174–183. https://doi.org/10.1007/BF02931255

31. Tsuboi, T., et al. (2023). Ebselen mitigates nephrotoxicity in drug-induced acute kidney injury via GPx-mimetic activity. *Pharmaceuticals*, 16(5), 687. https://doi.org/10.3390/ph16050687

32. Branco, V., Caito, S., Farina, M., Teixeira da Rocha, J. B., Aschner, M. (2017). Biomarkers of mercury toxicity: Past, present, and future trends. *Journal of Toxicology and Environmental Health*, Part B, 20(3), 119–154.

33. Halliwell, B. (2011). Free radicals and antioxidants – quo vadis? *Trends in Pharmacological Sciences*, 32(3), 125 130.